MOLECULAR AND CELLULAR BIOLOGY, Sept. 1996, p. 4915–4922 Vol. 16, No. 9
0270-7306/96/$04.00+0

Composite Patterns in Neutral/Neutral Two-Dimensional Gels Demonstrate Inefficient Replication Origin Usage

ROBERT F. KALEJTA AND JOYCE L. HAMLIN*

Department of Biochemistry, University of Virginia School of Medicine, Charlottesville, Virginia 22908

Received 1 May 1996/Returned for modification 12 June 1996/Accepted 24 June 1996

The neutral/neutral two-dimensional (2-D) gel replicon mapping technique has been used to great advantage to localize and characterize origins of replication. Interestingly, many yeast origins display a composite pattern consisting of both a bubble arc and a single-fork arc. Moreover, in every instance in which neutral/neutral 2-D gels have been used to analyze origins in higher eukaryotic cells, two or more adjacent fragments display these composite patterns. We believe that composite patterns signal inefficient origin usage in yeast cells because the replicators in question are not active in every cell cycle and in higher eukaryotic replicons because initiation sites are chosen from among many potential sites lying within a zone. However, others have suggested that the single-fork arcs in these composite gel patterns arise from nicking activity that converts replication bubbles to branched structures that comigrate with bona fide single forks. Here, we have used three different replicon mapping strategies to show that broken simian virus 40 replication bubbles trace unique arcs that are clearly distinguishable from classic, intact single forks. Thus, it is likely that composite 2-D gel patterns represent origins that are inefficiently utilized.

The replicon model proposes that a *trans*-acting factor (the initiator) interacts with a specific genetic element (the replicator) to effect local melting of the helix and subsequent initiation of nascent DNA chains (26). The more general term, origin, has been used to define the template positions at which nascent strands initiate (24). The replicon model predicts that (i) replicators should direct the autonomous replication of colinear sequences, (ii) replicator-containing sequences should be synthesized before any other fragments in a replicon, and (iii) the replicator should approximately colocalize with nascent-strand start sites. In virtually all bacterial, plasmid, viral, and yeast replicons, these conditions are met.

In higher eukaryotic replicons, the picture is less clear. For unknown reasons, genetic assays have not reliably uncovered specific sequences that are capable of reproducibly directing autonomous replication and which would therefore fit the definition of genetic replicators (but see references 22, 27, 39, 48, and 53). As a consequence, a number of physical mapping strategies have been developed to localize origins in higher eukaryotic genomes. However, the pictures painted by different origin mapping techniques are not entirely consistent with one another. The Chinese hamster dihydrofolate reductase (DHFR) domain, which has been analyzed by more techniques than any other, is a case in point.

Several physical mapping methods have been used to identify an initiation zone lying in the 55-kb region between the DHFR and 2BE2121 genes (1, 6–8, 19, 21, 28, 35, 49, 50). The results of two high-resolution intrinsic labelling approaches suggest that there are actually two preferred initiation sites or zones (termed ori-β and ori-γ) within the intergenic region that are separated by ~22 kb and that straddle a matrix attachment site (11). Measurements of leading-strand polarity in the Chinese hamster ovary DHFR domain also argue for the presence of two preferred sites or zones (19). More recent studies that measure either lagging-strand polarity or the size distribution of nascent DNA suggest that the great majority of initiations occur within a 500- to 2,000-bp zone encompassing ori-β (the ori-γ region was not examined in the latter two studies [8, 49]). Thus, all of these approaches are compatible with the presence of two preferred start sites at the ori-β and ori-γ positions.

Surprisingly, however, when the amplified and single-copy DHFR loci were examined in early S phase cells by the neutral/neutral two-dimensional (2-D) gel mapping technique (Fig. 1) (4), composite patterns consisting of complete bubble arcs and single-fork arcs were detected in every restriction fragment within the 55-kb intergenic region (although the concentration of replication bubbles seems to be higher in the central 30 to 35 kb) (12, 13, 15, 50). Thus, it appears that each fragment sometimes sustains an internal initiation event (giving rise to a bubble arc) but is often replicated passively by a replication fork emanating from an initiation site in a nearby fragment (giving rise to the single-fork arc). These data argue that the DHFR origin consists of a broad zone of potential initiation sites.

In fact, every higher eukaryotic origin that has been examined by the neutral/neutral 2-D gel technique displays a composite pattern in two or more adjacent fragments, suggesting that each represents an initiation zone (9, 20, 25, 30, 34, 45, 46). Moreover, several chromosomal autonomously replicating sequence elements in *Saccharomyces cerevisiae* display composite patterns in neutral/neutral 2-D gels (10, 16, 18, 31, 33, 42, 52), which could also indicate inefficient origin usage (although in the latter cases, it is clear that initiation sites lie very close to the genetic replicator itself and that a composite pattern is detected only in the autonomously replicating sequence-containing fragment itself).

In an effort to explain the composite 2-D gel patterns in each of these instances, the argument that replication bubbles broken at one or the other branch during isolation procedures would migrate as single forks has been invoked (8, 32). This phenomenon cannot explain the presence of bubble arcs in multiple adjacent fragments. However, significant breakage could explain why a preferred initiation site in the DHFR locus might have been overlooked on 2-D gels and why yeast chro-

* Corresponding author. Phone: (804) 924-5858. Fax: (804) 924-1789. Electronic mail address: jlh2d@virginia.edu.

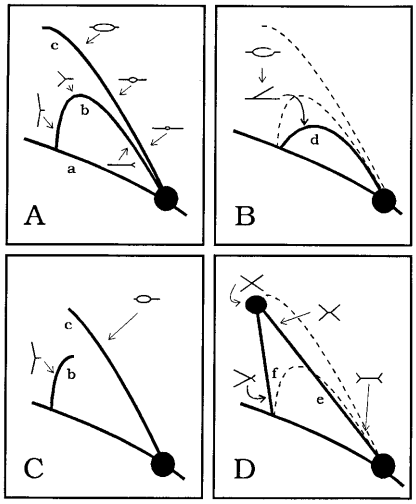

FIG. 1. Principle of the neutral/neutral 2-D gel replicon mapping method. A restriction digest is separated on an agarose gel in the first dimension on the basis of molecular mass. The resulting lane is excised, turned through 90°, and run in a second dimension that separates on the basis of both mass and shape. The digest is transferred to a membrane and hybridized with appropriate probes to detect the fragment of interest. (A) Curve a represents the arc of linear, nonreplicating fragments, and the large 1*n* spot corresponds to the nonreplicating component of any given probed fragment. Curve c corresponds to a fragment with a centered origin; curve b represents a fragment that is replicated passively by forks emanating from an outside origin. (B) Curve d represents a fragment containing a centered bubble that has suffered a break at one fork. (C) Off-centered origins would trace bubble arcs until one fork crosses a restriction site, after which the replication intermediates would migrate along the fork arc. (D) Fragments containing fixed centered termini (curve e) or random termination sites (curve f) would migrate as shown.

mosomal origins often display composite patterns (10, 16, 18, 31, 33, 42, 52).

In a study in which the destabilizing effects of various replication inhibitors on simian virus 40 (SV40) replication intermediates were examined in 2-D gels, we previously observed novel arcs that could have resulted from fragmented replication bubbles and which did not comigrate with single-fork arcs (26b). Using the SV40 replicon as a model, we show here that broken bubbles do not comigrate with bona fide single-forked structures on standard neutral/neutral 2-D gels but instead trace unique arcs whose shapes depend on the position of the bubble within the fragment. Using a three-dimensional (3-D) gel system (29) and the standard neutral/alkaline 2-D gel mapping method, we demonstrate that these novel arcs correspond to broken bubbles.

Thus, we conclude that composite patterns in neutral/neutral 2-D gels result from a combination of bona fide bubble arcs and single-fork arcs and probably result from inefficient origin usage. We further conclude that all three gel systems are extremely sensitive to minor structural changes in replication intermediates. In an accompanying report (26c), we utilize these observations to analyze the nature of replication intermediates in the amplified DHFR domain in CHOC 400 cells.

(This work fulfills part of the requirements for a Ph.D. degree in biochemistry from the University of Virginia for R. F. Kalejta.)

MATERIALS AND METHODS

Isolation of CHOC 400 replication intermediates. The methotrexate-resistant CHO cell line, CHOC 400 (40), was maintained in minimal essential medium (GIBCO) supplemented with nonessential amino acids and 10% bovine serum product (HyClone Laboratories) in an atmosphere of 5% CO_2. Cells were synchronized in G_0 by starving them for isoleucine for 45 h and were collected at the G_1/S boundary by incubation for 14 h in complete medium containing 400 μM mimosine (12). The mimosine was then removed and replaced with drug-free complete medium to allow entry into the S period. Ninety minutes later, at the peak of initiation in the DHFR locus (12), the cells were harvested and matrix-associated replication intermediates were isolated as previously described (14) by using *Xba*I to digest the DNA. Replication intermediates in the matrix-associated fraction were further purified by chromatography on benzoylated-naphthoylated-DEAE-cellulose (Sigma) prior to electrophoresis.

Viral propagation and isolation of replication intermediates. CV-1 cells were maintained as monolayer cultures in minimal essential medium supplemented with nonessential amino acids and 10% bovine serum product (HyClone) and were grown in an atmosphere of 5% CO_2. Cells were transfected with SV40 DNA (Bethesda Research Laboratories) by using Lipofectin (Bethesda Research Laboratories), and a virus stock was prepared by established procedures (3, 36). For experiments, ~0.5 PFU per cell were adsorbed to confluent 15-cm-diameter plates of CV-1 cells in 10 ml of minimal essential medium containing 1% serum for 1 h at 37°C, after which additional medium was added. Experiments began 24 h after infection.

Viral replication intermediates were isolated by the Hirt procedure (23), except that the lysis buffer contained 10 mM Tris-HCl (pH 8.0), 25 mM EDTA, 10 mM NaCl, and 0.6% sodium dodecyl sulfate and was supplemented with 100 μg of proteinase K (Amresco Laboratories) per ml just prior to use.

Hirt supernatants containing viral intermediates were incubated a second time with proteinase K (40 μg/ml for 15 min at 37°C), and the DNA was extracted twice with Tris-buffered phenol and twice with chloroform-isoamyl alcohol (24:1). Two volumes of −20°C absolute ethanol were added, and the DNA was collected immediately by centrifugation. The moist pellet from $\sim 1 \times 10^7$ to 2×10^7 cells was dissolved in 500 μl of 10 mM Tris-HCl (pH 7.4)–10 mM EDTA–10 mM NaCl, and the preparations were pooled and dialyzed for 2 h against the same buffer containing 50 μM phenylmethylsulfonyl fluoride at 4°C. DNA from $\sim 5 \times 10^6$ to 7.5×10^6 cells was digested at 37°C for 1 h with 50 U of the indicated restriction enzymes (Bethesda Research Laboratories) and 50 μg of RNase A (Sigma) per ml in a total volume of 300 μl. In some experiments (see the figure legends), 1 to 2 U of *Bal* 31 or 25 U of either mung bean or P1 nuclease were added to the restriction digest 10 min before completion. EDTA and NaCl were then added to 10 mM and 0.3 M, respectively, and the DNA was chromatographed on a 1-ml column of benzoylated-naphthoylated-DEAE-cellulose as described previously (14).

Gel electrophoresis. CHOC 400 or SV40 replication intermediates were separated on neutral/neutral 2-D gels exactly as described previously (14). The first dimensions of the two other gel separation methods used in this study were run in the same manner as those of the neutral/neutral 2-D gel technique (4). For neutral/alkaline gels (41), the first-dimension lane was excised, turned through 90°, and positioned at the top of a 1% agarose gel cast in water. The solidified gel with the first-dimension lane in place was initially equilibrated by soaking it twice for 45 min in 0.4 N NaOH to denature the replication intermediates and then by two 45-min incubations with alkaline electrophoresis buffer (40 mM NaOH, 1 mM EDTA). The gels were run at ~0.5 V/cm for 40 to 60 h at 4°C, and the buffer was changed once midway through the run. For 3-D gels (29), strips were excised from the second dimension of a neutral/neutral 2-D gel as described elsewhere (see the legend to Fig. 8) and were cast, equilibrated, and run in the same manner as that described above for the neutral/alkaline gel system.

After gel separations, replication intermediates were transferred to Hybond-N+ (Amersham Corp.) and hybridized with appropriate probes (see the figure legends) as previously described (12).

RESULTS

Broken replication bubbles trace unique arcs on 2-D gels. Typical composite neutral/neutral 2-D gel patterns of fragments XL and XD from the initiation locus of the DHFR domain are shown in Fig. 2. Fragment XL is ~4.5 kb long and contains the ori-β locus; fragment XD is 5.8 kb long and lies about 1.3 kb to the right (see Fig. 1A in reference 26c for a map of the DHFR domain). Both the bubble and the fork arc cover the range of molecular masses from the nonreplicating 1*n* spot to slightly less than 2*n*. The shapes of the presumed fork arcs in these fragments appear to be identical to that of fragment XA from the DHFR gene (Fig. 2), in which initiations have never been detected (12, 13, 15, 50). Thus, we have assumed that these arcs correspond to bona fide single-forked intermediates. Our interpretation of the composite patterns observed in fragments XD and XL is that each fragment sometimes sustains an active initiation event (contributing to the bubble arc) but is usually replicated passively from an origin emanating from other fragments in the intergenic region (thereby contributing to the single-fork arc).

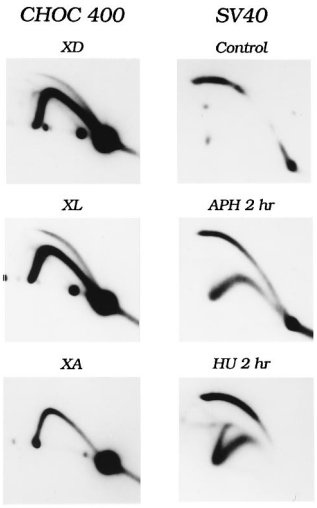

FIG. 2. Comparison of composite 2-D gel patterns from CHOC 400 cells with those of SV40 replication intermediates isolated from drug-treated cells. CHOC 400 cells were released from a mimosine-induced G_1/S block for 90 min, and replication intermediates were prepared as described previously (14), with *Xba*I being used to digest the DNA. The replication intermediates were separated on a 2-D gel, transferred to Hybond-N+, and hybridized successively with radioactive probes for fragments XD, XL, and XA (see Fig. 1 in reference 26c). CV-1 cells were infected with SV40 and, 24 h later, treated for 2 h either with no drug (control) or with 10 μg of aphidicolin (APH) (Sigma) per ml or 1 mM hydroxyurea (HU) (Sigma). Replication intermediates were then isolated and digested with *Bam*HI, which places the origin approximately in the center of the fragment (Fig. 3). After separation on a 2-D gel and transfer to Hybond-N+, the transfer was hybridized with radiolabelled viral DNA. The fragment sizes are as follows: XD, 4.6 kb; XL, 5.8 kb; XA, 5.5 kb; and SV40, 5.2 kb.

The 2-D gel patterns obtained after an examination of *Bam*HI-digested SV40 replication intermediates are quite different (Fig. 2). *Bam*HI cuts the SV40 genome at ~180° away from the origin, placing it near the center of the fragment (Fig. 3). The SV40 origin is used very efficiently and, as can be seen from Fig. 2, displays a single centered bubble arc. In all three SV40 examples in Fig. 2, the bubble arcs extend from 1*n* to 2*n* in the mass dimension; however, the strength of the hybridization signal is much greater toward the high end of the arc because of the greater mass of more fully replicated fragments

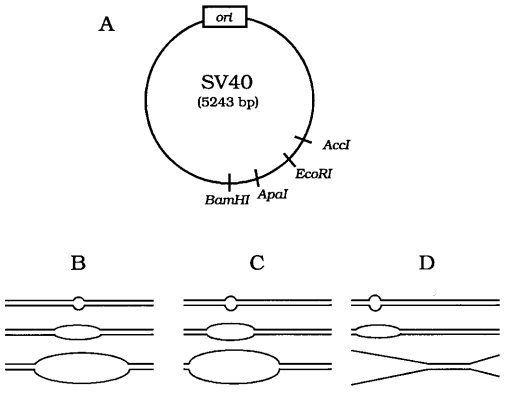

FIG. 3. Restriction map of the SV40 genome. (A) The viral genome is 5,243 residues long and is numbered from the *Bgl*I site at the origin. Relevant restriction sites are shown. By digesting them with different enzymes, identically sized fragments that differ in the positions of the origin can be generated. (B) A centered bubble (e.g., resulting from *Bam*HI digestion). (C and D) Off-centered bubbles (e.g., resulting from *Apa*I and *Eco*RI, respectively).

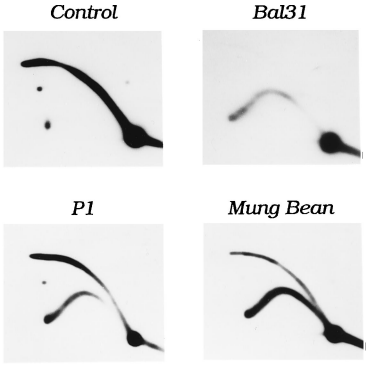

FIG. 4. Novel arcs can be generated in vitro by treating SV40 replication intermediates with a single-strand-specific nuclease. SV40 replication intermediates were isolated and digested with *Bam*HI, after which they were treated with *Bal* 31, P1, or mung bean nuclease for 10 min, as described in Materials and Methods. A transfer of the subsequent 2-D gel was hybridized with radiolabelled viral DNA.

as well as the nonlinear relationship between mass and migration rate on agarose gels.

After treatment of SV40-infected cells with aphidicolin for 2 h (Fig. 2), a novel arc that migrates quite differently than the single-fork arcs that characterize CHOC 400 fragments is detected. This same novel arc appears in the hydroxyurea-treated SV40 sample in which an apparently normal single-fork arc is also present, allowing a direct comparison of the different migration patterns. Since chain elongation inhibitors such as aphidicolin and hydroxyurea are thought to induce destabilization and breakage of replication intermediates (47), these data suggested to us that the novel arcs represent broken bubbles while the single-fork arc in hydroxyurea-treated samples may result from an aberrant form of rolling circle replication (26b). Furthermore, we have detected the novel arc when certain lots of *Bam*HI are used to digest replicating SV40 samples and have subsequently found that these preparations contain a nicking activity capable of relaxing supercoiled plasmids that lack a *Bam*HI site (data not shown).

To test directly whether the novel arcs correspond to bubbles that are converted to single-forked structures by nicking, SV40 replication intermediates were subjected to limited digestion in vitro with either *Bal* 31, P1, or mung bean nuclease. The single-strand-specific endonuclease activity of these enzymes should preferentially digest SV40 replication intermediates at the single-stranded regions of the fork itself (and presumably more often on the lagging strand). After further digestion to completion with a *Bam*HI preparation devoid of nicking activity, the products were analyzed on 2-D gels.

As can be seen in Fig. 4, partial digestion of SV40 with each of these enzymes gives rise to arcs whose shapes are quite similar to those of the novel arcs observed in the aphidicolin- and hydroxyurea-treated SV40 samples shown in Fig. 2. The samples treated with P1 and mung bean nucleases retain some of the intact bubble arc in this experiment, while the *Bal* 31 digest has proceeded further toward completion (note that *Bal* 31 also has exonuclease activity, which is largely suppressed under the conditions of this experiment). Presumably, any species that are doubly nicked appear as material migrating on the arc of linears at positions below the 1*n* spot in the mass dimension, although there is usually some low-molecular-weight material even in the untreated controls.

A mathematical model for the migratory behavior of broken bubbles on 2-D gels. Thus, fragments containing centered bub-

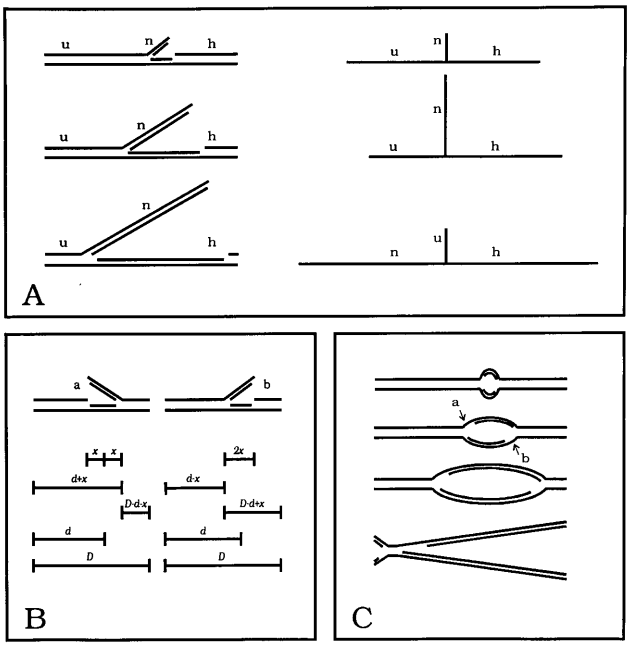

FIG. 5. A mathematical model predicts the migration patterns of broken bubbles on neutral/neutral 2-D gels. (A) Broken bubble structures for a fragment containing an off-centered origin are shown at different stages of replication. These structures are redrawn and simplified on the right to accentuate changes in symmetry as the bubble expands in each case. (B) A diagram of the two possible broken bubbles produced by nicks at either a or b. *D* connotes the length of the restriction fragment in base pairs, *d* is the distance from the end of the longer arm to the origin, and *x* is the distance traveled at any time by one replication fork (assuming bidirectional replication at equal rates). The model predicts that singly nicked bubbles will be most retarded on a 2-D gel when the newly generated arm (2*x*) is equal in length to the unreplicated arm to which it is attached. This situation occurs when $2x = D - d - x$ (nick at a) and when $2x = d - x$ (nick at b). Thus, each bubble should produce two broken bubble arcs that are maximally retarded at the value of *x* that solves the equations given above (if *D* and *d* are known). This point can be expressed as percent replicated ($2x/D$) or as ploidy [$1 + (2x/D)$]. (C) For circular replicons, double-forked termination structures are produced when the replication fork passes one of the restriction sites.

bles trace novel arcs on 2-D gels after being subjected to nicking with single-strand-specific nucleases. The question is whether these novel arcs really represent single-forked structures and, if so, why they migrate differently than normal replication forks on 2-D gels. The diagrams in Fig. 5A illustrate some possible nicked intermediates and lead to several testable predictions about the migration behavior of nicked bubbles.

A true single-forked replication intermediate is maximally retarded in the gel when the molecule is one-half replicated at a mass of 1.5*n*, because all three arms of the fork are equal at this point and the maximum average hydrodynamic volume is occupied. A fragment containing a broken bubble would also be maximally retarded if all three arms were the same length. However, this result is not possible, because as is indicated in Fig. 5A, the length of the newly generated arm produced by a nick (n) can never be as long as the hybrid arm (h) that contains both the parental duplex and the remaining half of the bubble (although the lengths can be quite close when a bubble almost reaches the end of a restriction fragment). We propose that a broken-bubble-containing fragment with a fixed origin will be maximally retarded when the sum of the differences in the lengths of the three arms is minimal. As the size of a small bubble increases, both the newly generated arm and the hybrid arm increase in length while the unreplicated arm decreases. Since the newly generated arm can never be equal in length to the hybrid arm, the differences among the three arms will be minimized when the length of the new arm (n) equals that of the unreplicated arm (u).

The parameters of this proposal are formalized in Fig. 5B, in which *D* is the length of the restriction fragment in question, *d* is the distance from the center of the bubble (origin) to the farthest end, and *x* represents the amount of DNA replicated by one fork (with the length of the newly generated arm becoming 2*x*). Since the bubble can be broken at either end (as shown in Fig. 5B, structures a or b), it follows that a linear template with a single fixed origin can actually trace two broken bubble arcs. A nick at point a gives an arc that reaches its maximum when $2x = D - d - x$; a nick at point b produces an arc whose maximum is reached when $2x = d - x$ (Fig. 5B). Only when the bubble is in the center of the fragment does solving these two equations for *x* give a single value at which broken bubble arcs should be maximally retarded; therefore, at this value, two identical novel arcs are detected. Thus, a *Bam*HI digest of SV40 should give a single arc (as it does [Fig. 4]), while other enzymes that move the origin away from the center of the fragment should produce two arcs.

When replication proceeds outward bidirectionally and at equal rates from the origin, the total distance travelled by the two forks is 2*x*. Therefore, the percentage of the fragment replicated at any moment becomes $2x/D$, and $1 + 2x/D$ is the corresponding ploidy. Eventually, the expanding bubble will reach the nearest end of the fragment, which would move the fragment from the bubble arc to the single-fork arc (termed a fork arc break [Fig. 1C]). If a circular molecule is analyzed, conversion to a termination structure (a termination arc break) would occur at this point (Fig. 1D and 5C). This conversion should occur at a ploidy of $1 + 2(D - d)/D$, because the fork reaches the nearest end when $d + x = D$ and the percent replicated becomes $2x/D$. Any given broken bubble, whether arising from a nick at point a or b in Fig. 5B, will ascend from the 1*n* spot and will terminate at the position of the fork arc break. The curve will be maximally retarded at the calculated ploidy, which depends on the position of the origin in the fragment. Note again that the distance travelled by a fragment in the first-dimension gel is approximately a function of the log of its mass, so fragments with a mass of 1.5*n* migrate closer to 2*n* than to 1*n*.

Verification of the model with the SV40 replicon. When this mathematical treatment is applied to a *Bam*HI digest of the SV40 genome, the two broken bubble arcs are predicted to be maximally retarded at molecular masses of 1.34*n* and 1.32*n* according to the following relationships. For $D = 5{,}243$ and $d = 2{,}710$, one broken bubble arc will be maximally retarded when $2x = d - x$ or $2x = 2{,}710 - x$. Solving for *x* gives a value of 903, and since the percent replicated is $2x/D$, or 1,806/5,243, this value corresponds to 1.34*n*. The point of maximal retardation of the second broken bubble can be calculated by the relationship $2x = D - d - x$ in a similar fashion and was found to be 1.32*n*.

Furthermore, the break that occurs when one replication fork transgresses the nearest restriction site should occur when $x = D - d$. Solving for *x* and converting to ploidy gives a value of 1.97*n*. In fact, only a single broken bubble arc is observed in the *Bam*HI digest shown in Fig. 4, and it probably consists of the two similarly migrating arcs predicted by the model. Furthermore, the termination arc break in a *Bam*HI digest is so close to one end that it would be virtually undetectable, which appears to be the case.

Figure 6 (upper right panel) shows the approximate pattern of broken bubble arcs expected from an *Eco*RI digest, which

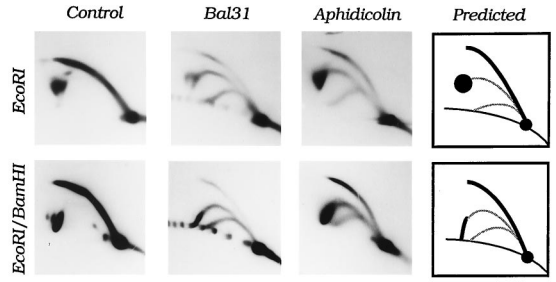

FIG. 6. Testing the model on the SV40 replicon. SV40 replication intermediates were isolated from drug-free or aphidicolin-treated CV-1 cells. The DNA samples were digested either with *Eco*RI, which positions the origin off center, or with *Eco*RI-*Bam*HI, which reduces the size of the bubble-containing fragment and moves the origin closer toward the center (Fig. 3). An aliquot of the drug-free control DNA was then treated with *Bal* 31 in vitro. Transfers of the resulting gel were hybridized with radiolabelled SV40 DNA. The panel on the right of each row is a diagram of the 2-D gel patterns predicted by the model for the two different digests (see text).

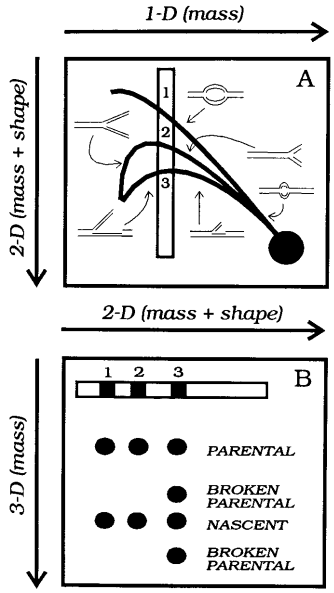

FIG. 7. The 3-D gel technique. (A) The first two dimensions are identical to the standard neutral/neutral 2-D gel separation conditions (4). After the second dimension, fragments with an active origin of replication trace a bubble arc (arc 1), fragments replicated passively by a single fork trace a fork or simple Y arc (arc 2), and broken bubbles trace distinct arcs beneath the fork arc whose position in the gel depends upon the position of the origin in the fragment (arc 3). (B) Gel slices taken from various positions along the mass dimension in the 2-D gel are turned through 90° and cast at the top of the third, alkaline gel. Bubbles (1), forks (2), and broken bubbles (3) yield identically sized parental and nascent fragments. However, broken bubbles additionally display novel spots that represent broken parental strands.

generates a full-length fragment with an off-centered bubble. The model predicts that the two broken bubbles from this template should be maximally retarded at masses of 1.44*n* (7.6 kb) and 1.23*n* (6.4 kb) and that a termination arc break should occur at 1.7*n* (9 kb).

The other three panels in the top row of Fig. 6 show the actual 2-D gel patterns obtained from the *Eco*RI-digested SV40 DNA (control) and from samples additionally treated either with *Bal* 31 in vitro or with aphidicolin for 2 h in vivo. The *Eco*RI-digested control DNA generates a bubble arc that extends almost to the 2*n* position (theoretically ~9 kb), at which point one fork passes an *Eco*RI site and the bubble-containing fragment is converted to a termination structure with two converging forks (see the diagrams in Fig. 1, 3, and 5C). Treatment of the DNA with *Bal* 31 generates two broken bubble arcs that are maximally retarded at ~8.5 and 6.7 kb (assessed with a 1-kb ladder included in the *Bal* 31 digest and visible on the arc of linears in Fig. 6). These sizes are quite consistent with those predicted by the model (7.6 and 6.4 kb), given that there is some effect of shape even in the first-dimension gel (4, 29). This effect can be detected in Fig. 2, in which the SV40 bubble arcs are seen to extend slightly beyond 2*n* in the mass dimension, even though they actually should not have a mass greater than 2*n*. The DNA prepared from cells treated with aphidicolin displays an almost identical 2-D gel pattern.

When SV40 replication intermediates are treated with both *Bam*HI and *Eco*RI, the origin-containing fragment is shortened and the origin again occupies an off-center position. The model predicts broken bubble arcs with maxima at 1.4*n* (6.3 kb) and 1.26*n* (5.7 kb), with a fork arc break at 1.8*n* (8.1 kb). The actual patterns of these *Bam*HI-*Eco*RI fragments after treatment with either *Bal* 31 or aphidicolin are shown in the two center panels of Fig. 6. The broken bubble arcs peak at ~7 and 5.8 kb, and the fork arc break occurs at about 8 kb.

Thus, the model makes reasonably accurate predictions of the migration patterns of broken bubble arcs on 2-D gels and suggests the possibility that broken bubble arcs could be used to map the positions of origins in a restriction fragment. In the accompanying report (26c), we have applied this method to an analysis of the DHFR origin in CHOC 400 cells in order to search for a highly preferred initiation site near ori-β.

3-D gels distinguish broken bubbles and single-fork arcs. Liang and Gerbi developed a novel 3-D gel separation strategy that, in principle, should be able to detect broken bubbles if they exist in a DNA preparation (29). In this technique (Fig. 7), a standard neutral/neutral 2-D gel is run; strips are then excised from the gel at positions of known molecular mass and are turned through 90° and run in a third, alkaline dimension to release nascent strands from the template. This procedure allows the vertical separation of parental and nascent strands on the basis of their different sizes as well as the horizontal separation of the bubble and fork arc in the second dimension. This technique can detect broken bubbles by two mechanisms. Broken parental fragments, which will necessarily be smaller than the full-length parental template, will migrate as unique spots in the third dimension, and these fragments should be distinguishable from both intact parental and nascent strands. Furthermore, a hybridization probe from the center of a fragment should not detect any small nascent strands released from the fork arc unless the fork arc contains broken bubbles (29).

When the initiation zone of a *Sciara coprophila* puff was analyzed by this technique, Liang and Gerbi could not detect any novel spots arising from the single-fork arc that could represent fragmented template strands arising from broken bubbles (29). They therefore concluded that their preparations of replication intermediates probably did not contain significant quantities of broken bubbles. However, they did not actually define the positions of broken bubbles in their gel system, and we have presented evidence above that broken bubbles do not comigrate with fork arcs; rather, they appear to trace novel arcs whose positions depend on the placement of the origin within the fragment. These novel arcs are assumed to correspond to broken bubbles because they can be created by single-strand-specific nucleases and by treatment of SV40-

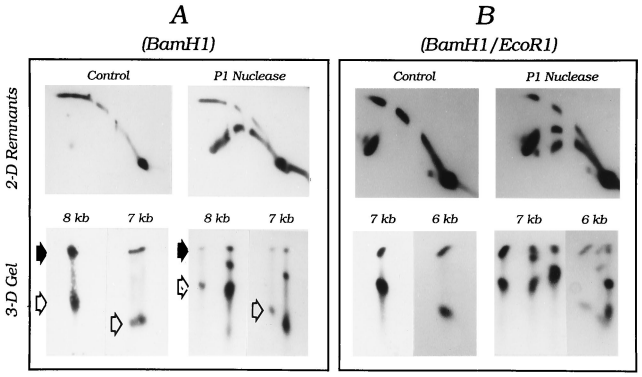

FIG. 8. 3-D gels confirm the structures of broken bubbles. SV40 replication intermediates were digested with *Bam*HI or BamHI-EcoRI, and the samples were further subjected to partial digestion with P1 nuclease. The products were separated on a 3-D gel, transferred to a membrane, and probed with radiolabelled total SV40 DNA. (A) The remnants of the 2-D gel display the expected patterns of bubble arcs and, with nuclease treatment, broken bubbles. (B) In the 3-D gel, the excised lanes from the control sample yield parental and nascent-strand spots, while the P1 nuclease-treated samples yield two additional spots above and below the nascent-strand signal which correspond to the broken template fragments. Note that in panel A, the gel containing the nuclease-treated samples was not run as far as the one with the control samples (see text).

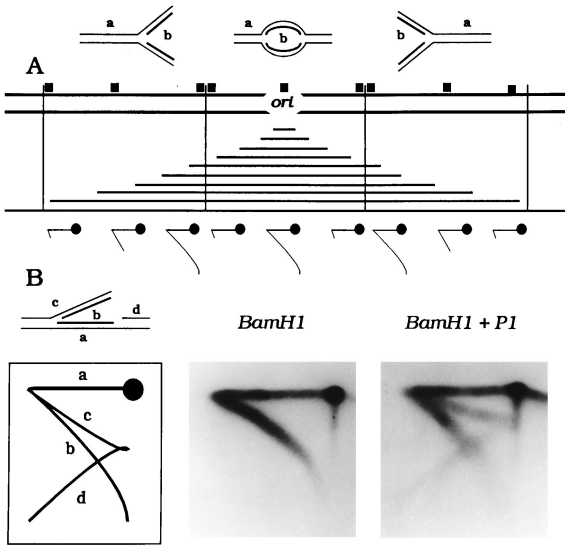

FIG. 9. Neutral/alkaline 2-D gels also detect broken parental fragments. SV40 replication intermediates were digested with *Bam*HI with or without P1 nuclease. The resulting samples were separated on a standard neutral/alkaline gel, blotted, and probed with radiolabelled SV40 DNA. (A) Principle of the neutral/alkaline gel technique. (B) The predicted neutral/alkaline gel pattern of a centered broken bubble and the resulting gel patterns of BamHI-digested SV40 replication intermediates with and without P1 nuclease treatment.

infected cells with aphidicolin, which has been shown to fragment and destabilize replication intermediates (47).

To confirm this assumption, SV40 replication intermediates were partially digested with the single-strand-specific nuclease, P1, were then digested to completion with either *Bam*HI alone or in combination with *Eco*RI, and were subjected to 3-D gel electrophoresis (Fig. 7 and 8). After a standard neutral/neutral 2-D gel run, 5-mm-wide vertical strips were excised at the 8- and 7-kb positions in the *Bam*HI digest and at the 7- and 6-kb positions in the *Bam*HI-*Eco*RI digests. The strips were then turned through 90° and run in the third, alkaline dimension. After being blotted to a membrane, both the 3-D gel and the remainder of the 2-D gel were probed with randomly primed total SV40 DNA.

In the 2-D gels from which the strips were excised, control samples show only bubble arcs; nuclease treatment produces the novel arcs that are predicted by the model to correspond to broken bubble arcs. Control samples separated in the third (alkaline) dimension (Fig. 8) yield a full-length spot, which undoubtedly corresponds to the template, as well as a smaller spot whose size approximates that expected for nascent strands on the basis of the size of the starting replication bubble. This spot decreases in mobility as the extent of replication increases, as would be expected of nascent strands. In the nuclease-treated samples, the bubble arc gives rise to the same size parental and nascent bands as those in the control; however, the novel (broken bubble) arc gives rise not only to these spots but also to two additional bands whose sizes approximately correspond to the two broken parental fragments from a single-nicked bubble (see the diagram in Fig. 5). (Note that the control and nuclease-treated DNAs in the 3-D gels in Fig. 8A ran different distances; the solid and open arrows signify the template and nascent strands in each case.)

In independent studies, we have been able to assign individual spots to nascent DNA strands by analyzing SV40 replication intermediates that were briefly labelled in vivo with [^{3}H]thymidine (26a). Together with the data obtained by probing with ^{32}P-labelled SV40 DNA (Fig. 8), it is therefore possible to deduce the origin of each of the bands in these gels. On the basis of the 3-D gel analysis, we conclude that the novel arcs travelling below the standard single-fork arc on 2-D gels result from bubbles that have been broken at one of the forks.

Standard neutral/alkaline gels also distinguish broken bubbles and classic single-forked replication intermediates. Many of the initiation zones that have been identified by the neutral/neutral 2-D gel method have also been characterized with the neutral/alkaline 2-D gel technique (41). This method determines fork direction through a fragment of interest by determining the sizes of nascent strands detected with end and centered probes (Fig. 9). This method has been used to confirm the prediction that forks move in both directions through fragments residing in initiation zones (12, 15, 30, 46, 50). In none of these instances was any novel arc detected that did not conform to one of the patterns shown below the diagram in Fig. 9A. However, since it has been suggested that broken bubbles could complicate the interpretation of 2-D gels (8, 32), we also characterized the migration pattern of broken bubbles on neutral/alkaline gels.

In this technique, samples are separated in the first, neutral dimension by size; the second dimension also separates by size but is run under alkaline conditions to release nascent strands from the template. Thus, the nascent strands trace a descending arc from the horizontal template band. Were there to be a significant number of broken bubbles in a fragment with a centered origin, two new arcs should be generated from the two parts of the broken parental strand (Fig. 9B). The larger part containing the origin sequence itself would range in size from slightly more than 50% for the smallest bubbles to almost 100% of the full-length fragment; the smaller template fragment would range from just less than 50% to almost 0% of the full-length single-stranded template. When the origin is not in the center of the fragment, the bubble can be broken at one or the other end, resulting in two novel arcs for each end (a total of four). Bubbles broken at both ends would yield less-than-full-length fragments that would migrate below and to the right of the 1*n* spot.

To test these predictions, replicating SV40 DNA was par-

tially digested with P1 nuclease and linearized with *Bam*HI, which positions the origin in the center. Digests were then separated on a neutral/alkaline 2-D gel. Transfers of the digests were probed with ^{32}P-labelled total SV40 DNA in order to illuminate the full spectrum of intermediates (equivalent to using a combination of end and centered probes).

As can be seen from Fig. 9B, control samples that were not treated with P1 nuclease trace a complete diagonal, indicating that replication bubbles of all sizes were present in the sample. After treatment with P1 nuclease, however, novel arcs whose shapes exactly mimic those predicted for broken centered bubbles appear. Since neither of these arcs has been detected in any of the neutral/alkaline 2-D gel analyses of initiation zones (13, 15, 30, 46, 50), it is unlikely that broken bubbles have been overlooked in those studies. Digests that move the origin away from the center of the fragment also produce the predicted neutral/alkaline gel patterns (data not shown).

DISCUSSION

We have addressed one of the possible reasons for the presence of composite patterns in neutral/neutral 2-D gels, namely, that replication bubbles can be nicked during preparation and converted to single-forked structures that comigrate with legitimate single-fork arcs. Following up on the observation that destabilized SV40 replicons yield novel arcs that could represent broken bubbles, we have shown directly that cleavage with single-strand-specific nucleases converts SV40 bubbles into single-forked structures that trace unique arcs on neutral/neutral 2-D gels (Fig. 4). A model which predicts that off-centered bubbles actually produce two different broken bubble arcs has been developed. The model was validated by showing that SV40 replication intermediates treated either in vitro with nucleases or in vivo with aphidicolin generate novel arcs that migrate at positions distinctly different from those of classic single forks (Fig. 6). With some minor modifications, our model is also able to predict the structures of broken bubbles produced from a unidirectional origin in a bacterial plasmid (37, 38). Furthermore, the migration behavior of the pair of arcs from any single fixed origin position differs from that of a pair generated by fragments with the origin in a different position. These observations form the basis of a broken bubble assay, which we have used to search for a preferred initiation site in the DHFR ori-β locus in the accompanying study (26c).

It should be emphasized that our model only addresses the behavior of broken bubbles up to the point at which one fork transgresses the nearest restriction site, which, in intact replication intermediates, would result in a fork arc break. After conversion of the bubble to a fork, a single nick would result in linear fragments with masses of 1*n* and less. Also, note that the migration of replication intermediates on 2-D gels is dependent not only on shape but also on fragment length and gel conditions. Because of this, the shapes of the patterns traced by both destabilized and classic replication intermediates differ slightly on gels run in different laboratories or on different DNA samples.

We confirmed that the novel arcs generated by single-strand-specific nucleases correspond to broken bubbles by the 3-D gel technique, which allows direct observation of the two fragmented template strands in the third dimension and confirms that only the novel (broken bubble) arc in the second dimension gives rise to these fragments (Fig. 8). Finally, application of the standard neutral/alkaline 2-D gel method to nicked SV40 replication intermediates produced distinctive and predictable patterns that are clearly distinguishable from patterns obtained with classic bubbles or single-forked intermediates (Fig. 9).

In total, our data argue that composite patterns on neutral/neutral 2-D gels do not arise from broken bubbles (31, 32). Therefore, composite patterns probably result from inefficient origin usage. In the case of some yeast autonomously replicating sequence elements (10, 16, 18, 31, 33, 42, 52), the presence of a single-fork arc in an autonomously replicating sequence-containing fragment suggests that the origin does not fire in every cell cycle. In higher eukaryotic origins, such as the CHO DHFR (12, 13, 15, 50) and human rDNA loci (34), composite patterns probably arise because initiation sites in this locus are chosen from many potential sites distributed throughout a broad zone, as we and others have suggested (12, 30, 34, 46). However, in none of these cases has the presence of somewhat preferred sites been ruled out.

Finally, the present study illuminates the power of 2-D gels to discriminate among replication intermediates with identical masses but subtle structural differences. In fact, various 2-D gel techniques have been used for years to differentiate among DNA molecules with different topologies and degrees of catenation (2, 43, 44, 51). More recently, the standard neutral/neutral 2-D gel approach has been shown to be sensitive to small changes in the structures of intermediates formed during unidirectional replication of pBR322 (37, 38). Additionally, replication intermediates from *Schizosaccharomyces pombe*, *S. cerevisiae*, the CHOC 400 DHFR locus, and the human rDNA locus were recently shown to comigrate on 2-D gels, attesting to the identity of their structures (5). For these reasons, we predict that the migration patterns of fragments containing noncanonical replication intermediates (for example, microbubbles [17]) would be easily distinguished from those of the classic intermediates pictured in Fig. 1.

In an accompanying report (26c), we have applied the broken bubble assay and a novel stop-and-go-alkaline gel technique to analyze replication intermediates in the CHO DHFR locus. The data from that study provide strong support for a model in which initiation sites are chosen from many potential sites within a broad zone.

ACKNOWLEDGMENTS

We thank Hong-Bo Lin and Pieter Dijkwel, who have contributed valuable advice and aid throughout the course of this project. In particular, Pieter Dijkwel carried out the neutral/neutral 2-D gel analysis of CHOC 400 replication intermediates in the experiment pictured in Fig. 2. We are also very grateful to Carlton White and Kevin Cox for enthusiastic and expert technical assistance.

This study was supported by NIH grant R01 GM26108 to J.L.H. R.F.K. was supported by NIH training grant T32 GM08136.

REFERENCES

1. **Anachkova, B., and J. L. Hamlin.** 1989. Replication in the amplified dihydrofolate reductase domain in CHO cells may initiate at two distinct sites, one of which is a repetitive sequence element. Mol. Cell. Biol. **9:**532–540.
2. **Bell, L., and B. Byers.** 1983. Separation of branched from linear DNA by two-dimensional gel electrophoresis. Anal. Biochem. **130:**527–535.
3. **Black, P. H., E. M. Crawford, and L. V. Crawford.** 1964. The purification of simian virus 40. J. Virol. **24:**381–387.
4. **Brewer, B. J., and W. L. Fangman.** 1987. The localization of replication origins on ARS plasmids in S. cerevisiae. Cell **51:**463–471.
5. **Brun, C., P. A. Dijkwel, R. D. Little, J. L. Hamlin, C. L. Schildkraut, and J. A. Huberman.** 1995. Yeast and mammalian replication intermediates migrate similarly in two-dimensional gels. Chromosoma **104:**92–102.
6. **Burhans, W. C., J. E. Selegue, and N. H. Heintz.** 1986. Replication intermediates formed during initiation of DNA synthesis in methotrexate-resistant CHOC 400 cells are enriched for sequences derived from a specific, amplified restriction fragment. Biochemistry **25:**441–449.
7. **Burhans, W. C., J. E. Selegue, and N. H. Heintz.** 1986. Isolation of the origin of replication associated with the amplified Chinese hamster dihydrofolate reductase domain. Proc. Natl. Acad. Sci. USA **83:**7790–7794.

8. **Burhans, W. C., L. T. Vassilev, M. S. Caddle, N. H. Heintz, and M. L. DePamphilis.** 1990. Identification of an origin of bidirectional DNA replication in mammalian chromosomes. Cell **62:**955–965.
9. **Delidakis, C., and F. C. Kafatos.** 1989. Amplification enhancers and replication origins in the autosomal chorion gene cluster of Drosophila. EMBO J. **8:**891–901.
10. **Dershowitz, A., and C. S. Newlon.** 1993. The effect on chromosome stability of deleting replication origins. Mol. Cell. Biol. **13:**391–398.
11. **Dijkwel, P. A., and J. L. Hamlin.** 1988. Matrix attachment regions are positioned near replication initiation sites, genes, and an interamplicon junction in the amplified dihydrofolate reductase domain of Chinese hamster ovary cells. Mol. Cell. Biol. **8:**5398–5409.
12. **Dijkwel, P. A., and J. L. Hamlin.** 1992. Initiation of DNA replication in the dihydrofolate reductase locus is confined to the early S period in CHO cells synchronized with the plant amino acid mimosine. Mol. Cell. Biol. **12:**3715–3722.
13. **Dijkwel, P. A., and J. L. Hamlin.** 1995. The Chinese hamster dihydrofolate reductase origin consists of multiple potential nascent-strand start sites. Mol. Cell. Biol. **15:**3023–3031.
14. **Dijkwel, P. A., J. P. Vaughn, and J. L. Hamlin.** 1991. Mapping of replication initiation sites in mammalian genomes by two-dimensional gel analysis: stabilization and enrichment of replication intermediates by isolation on the nuclear matrix. Mol. Cell. Biol. **11:**3850–3859.
15. **Dijkwel, P. A., J. P. Vaughn, and J. L. Hamlin.** 1994. Replication initiation sites are distributed widely in the amplified CHO dihydrofolate reductase domain. Nucleic Acids Res. **22:**4989–4996.
16. **Ferguson, B. M., B. J. Brewer, A. E. Reynolds, and W. L. Fangman.** 1991. A yeast origin of replication is activated late in S phase. Cell **65:**507–515.
17. **Gaudette, M. F., and R. M. Benbow.** 1986. Replication forks are underrepresented in chromosomal DNA of Xenopus laevis embryos. Proc. Natl. Acad. Sci. USA **83:**5953–5957.
18. **Greenfeder, S. A., and C. S. Newlon.** 1992. A replication map of a 61-kb circular derivative of Saccharomyces cerevisiae chromosome III. Mol. Biol. Cell **3:**999–1013.
19. **Handeli, S., A. Klar, M. Meuth, and H. Cedar.** 1989. Mapping replication units in animal cells. Cell **57:**909–920.
20. **Heck, M. M., and A. C. Spradling.** 1990. Multiple replication origins are used during Drosophila chorion gene amplification. J. Cell Biol. **110:**903–914.
21. **Heintz, N. H., and J. L. Hamlin.** 1982. An amplified chromosomal sequence that includes the gene for dihydrofolate reductase initiates replication within specific restriction fragments. Proc. Natl. Acad. Sci. USA **79:**4083–4087.
22. **Heinzel, S. S., P. J. Krysan, C. T. Tran, and M. P. Calos.** 1991. Autonomous DNA replication in human cells is affected by the size and the source of the DNA. Mol. Cell. Biol. **11:**2263–2272.
23. **Hirt, B.** 1967. Selective extraction of polyoma DNA from infected mouse cell cultures. J. Mol. Biol. **26:**365–369.
24. **Huberman, J. A., and A. D. Riggs.** 1968. On the mechanism of DNA replication in mammalian chromosomes. J. Mol. Biol. **32:**327–341.
25. **Hyrien, O., and M. Mechali.** 1993. Chromosomal replication initiates and terminates at random sequences but at regular intervals in the ribosomal DNA of Xenopus early embryos. EMBO J. **12:**4511–4520.
26. **Jacob, F., and S. Brenner.** 1963. Sur la régulation de la synthèse du DNA chez les bactéries: l'hypothèse du replicon. C. R. Acad. Sci. **246:**298–300.

26a. **Kalejta, R. F.** Unpublished data.

26b. **Kalejta, R. F., and J. L. Hamlin.** Submitted for publication.

26c. **Kalejta, R. F., H.-B. Lin, P. A. Dijkwel, and J. L. Hamlin.** 1996. Characterizing replication intermediates in the amplified CHO dihydrofolate reductase domain by two novel gel electrophoretic techniques. Mol. Cell. Biol. **16:**4923–4931.

27. **Krysan, P. J., and M. P. Calos.** 1991. Replication initiates at multiple locations on an autonomously replicating plasmid in human cells. Mol. Cell. Biol. **11:**1464–1472.
28. **Leu, T. H., and J. L. Hamlin.** 1989. High-resolution mapping of replication fork movement through the amplified dihydrofolate reductase domain in CHO cells by in-gel renaturation analysis. Mol. Cell. Biol. **9:**523–531.
29. **Liang, C., and S. A. Gerbi.** 1994. Analysis of an origin of DNA amplification in *Sciara coprophila* by a novel three-dimensional gel method. Mol. Cell. Biol. **14:**1520–1529.
30. **Liang, C., J. D. Spitzer, H. S. Smith, and S. A. Gerbi.** 1993. Replication initiates at a confined region during DNA amplification in Sciara DNA puff II/9A. Genes Dev. **7:**1072–1084.
31. **Liang, C., M. Weinreich, and B. Stillman.** 1995. ORC and Cdc6p interact and determine the frequency of initiation of DNA replication in the genome. Cell **81:**667–676.
32. **Linskens, M. H., and J. A. Huberman.** 1990. Ambiguities in results obtained with 2D gel replicon mapping techniques. Nucleic Acids Res. **18:**647–652.
33. **Linskens, M. H. K., and J. A. Huberman.** 1988. Organization of replication of ribosomal DNA in *Saccharomyces cerevisiae*. Mol. Cell. Biol. **8:**4927–4935.
34. **Little, R. D., T. H. Platt, and C. L. Schildkraut.** 1993. Initiation and termination of DNA replication in human rRNA genes. Mol. Cell. Biol. **13:**6600–6613.
35. **Ma, C., T.-H. Leu, and J. L. Hamlin.** 1990. Multiple origins of replication in the dihydrofolate reductase amplicons of a methotrexate-resistant Chinese hamster cell line. Mol. Cell. Biol. **10:**1338–1346.
36. **Martin, M. A., and D. Axelrod.** 1969. SV40 gene activity during lytic infection and in a series of SV40 transformed mouse cells. Proc. Natl. Acad. Sci. USA **64:**1203–1210.
37. **Martin, P. L., P. Hernandez, R. M. Martinez, and J. B. Schvartzman.** 1991. Unidirectional replication as visualized by two-dimensional agarose gel electrophoresis. J. Mol. Biol. **220:**843–853.
38. **Martin, P. L., P. Hernandez, R. M. Martinez, and J. B. Schvartzman.** 1992. Initiation of DNA replication in ColE1 plasmids containing multiple potential origins of replication. J. Biol. Chem. **267:**22496–22505.
39. **McWhinney, C., and M. Leffak.** 1990. Autonomous replication of a DNA fragment containing the chromosomal replication origin of the human c-myc gene. Nucleic Acids Res. **18:**1233–1242.
40. **Milbrandt, J. D., N. H. Heintz, W. C. White, S. M. Rothman, and J. L. Hamlin.** 1981. Methotrexate-resistant Chinese hamster ovary cells have amplified a 135-kilobase-pair region that includes the dihydrofolate reductase gene. Proc. Natl. Acad. Sci. USA **78:**6043–6047.
41. **Nawotka, K. A., and J. A. Huberman.** 1988. Two-dimensional gel electrophoretic method for mapping DNA replicons. Mol. Cell. Biol. **8:**1408–1413.
42. **Rivier, D. H., and J. Rine.** 1992. An origin of DNA replication and a transcription silencer require a common element. Science **256:**659–663.
43. **Serwer, P.** 1985. Two-dimensional agarose gel electrophoresis without gel manipulation. Anal. Biochem. **144:**172–178.
44. **Serwer, P., R. H. Watson, and S. J. Hayes.** 1987. Multidimensional analysis of intracellular bacteriophage T7 DNA: effects of amber mutations in genes 3 and 19. J. Virol. **61:**3499–3509.
45. **Shinomiya, T., and S. Ina.** 1991. Analysis of chromosomal replicons in early embryos of Drosophila melanogaster by two-dimensional gel electrophoresis. Nucleic Acids Res. **19:**3935–3941.
46. **Shinomiya, T., and S. Ina.** 1993. DNA replication of histone gene repeats in *Drosophila melanogaster* tissue culture cells: multiple initiation sites and replication pause sites. Mol. Cell. Biol. **13:**4098–4106.
47. **Snapka, R. M., C. G. Shin, P. A. Permana, and J. Strayer.** 1991. Aphidicolin-induced topological and recombinational events in simian virus 40. Nucleic Acids Res. **19:**5065–5072.
48. **Sudo, K., M. Ogata, Y. Sato, A. S. Iguchi, and H. Ariga.** 1990. Cloned origin of DNA replication in c-myc gene can function and be transmitted in transgenic mice in an episomal state. Nucleic Acids Res. **18:**5425–5432.
49. **Vassilev, L. T., W. C. Burhans, and M. L. DePamphilis.** 1990. Mapping an origin of DNA replication at a single-copy locus in exponentially proliferating mammalian cells. Mol. Cell. Biol. **10:**4685–4689.
50. **Vaughn, J. P., P. A. Dijkwel, and J. L. Hamlin.** 1990. Replication initiates in a broad zone in the amplified CHO dihydrofolate reductase domain. Cell **61:**1075–1087.
51. **Wasserman, S. A., J. M. Dungan, and N. R. Cozzarelli.** 1985. Discovery of a predicted DNA knot substantiates a model for site-specific recombination. Science **229:**171–174.
52. **Wohlgemuth, J. G., G. H. Bulboaca, M. Moghadam, M. S. Caddle, and M. P. Calos.** 1994. Physical mapping of origins of replication in the fission yeast Schizosaccharomyces pombe. Mol. Biol. Cell **5:**839–849.
53. **Wu, C., P. Friedlander, C. Lamoureux, H. M. Zannis-Hadjopoulos, and G. B. Price.** 1993. cDNA clones contain autonomous replication activity. Biochim. Biophys. Acta **1174:**241–257.